ELSEVIER

Journal of Photochemistry and Photobiology
A: Chemistry 88 (1995) 93–104

Journal of PHOTOCHEMISTRY AND PHOTOBIOLOGY A: CHEMISTRY

Fluorescence and intersystem crossing from the twisted intramolecular charge transfer (TICT) state of bianthryl in the presence of inorganic ions in polar solvents

Marek Mac [a,1], Jan Najbar [b], Jakob Wirz [a]

[a] *Institut für Physikalische Chemie, Universität Basel, Klingelbergstrasse 80, CH-4056 Basel, Switzerland*
[b] *Faculty of Chemistry, Jagiellonian University, 30-060 Kraków, Ingardena 3, Poland*

Received 10 October 1994; accepted 22 November 1994

Abstract

Quenching of bianthryl (BA) fluorescence by thiocyanide (SCN^-), bromide (Br^-) and iodide (I^-) anions in acetonitrile and alcohols was investigated. The quantum yield of BA triplet formation as a function of the quencher concentration was determined using flash photolysis. A kinetic scheme is proposed to model the processes following the fluorescence quenching of BA. It is found that the radical pairs produced by electron transfer quenching of the excited state of anthracene and of the twisted intramolecular charge transfer (TICT) state of BA recombine to the triplet and ground states with different efficiencies: ground state recovery seems to be more important in the case of BA. The discussion highlights the role of spin–orbit coupling in intersystem crossing and of the solvent polarity in the forward and reverse electron transfer processes.

Keywords: Electron transfer; Intersystem crossing; Heavy-atom effect; Fluorescence quenching; Bianthryl; Twisted intramolecular charge transfer states

1. Introduction

Bianthryl (BA) exhibits dual fluorescence in polar solvents, which is interpreted in terms of a twisted intramolecular charge transfer (TICT) state. This was originally proposed by Grabowski et al. [1] to explain the dual fluorescence of *N,N*-dimethylaminobenzonitrile (DMABN). The TICT hypothesis was later verified by time-resolved fluorescence and absorption spectroscopy [2–6]. Since the TICT states consist of two linked radical ions of opposite charge at close spatial separation, they possess large dipole moments.

Several studies have dealt with the quenching of TICT excited states by inorganic molecules. Kołos and Grabowski [7] found that the fluorescence of DMABN in water was affected by small inorganic anions, such as OH^-, F^- and Cl^-, which are usually ineffective as quenchers of excited aromatic molecules [8]. They used the concept of hard and soft bases and acids to explain these findings. The fluorescence quenching of BA by hydrogen ions in acetonitrile and methanol was investigated by Shizuka et al. [9].

The fluorescence quenching of aromatic molecules (A) by inorganic anions (X^-) has been the subject of many investigations [8,10]. Recently, we investigated the effect of the fluorescence quenching of aromatic molecules by inorganic anions on the formation of molecular triplet states and radical products (A^-, X and X_2^-) in polar solvents using the technique of flash photolysis [10]. The results confirmed that the quenching was due to electron transfer. It was shown that the interception of geminal radical pairs (A^-/X) by excess anions X^- plays an important role by modifying the rates of intersystem crossing (ISC) and reverse charge transfer in the radical pairs. These findings agree with earlier results for the quenching of the triplet states of ketones and quinones by inorganic anions in water [11].

The fluorescence quenching of aromatic molecules in bimolecular reactions, particularly in systems containing heavy atoms, was also interpreted in terms of an exciplex model [12]. In this model, the relaxation processes from the excited singlet state, internal con-

[1] Present address: Faculty of Chemistry, Jagiellonian University, 30-060 Kraków, Ingardena 3, Poland.

1010-6030/95/$09.50
SSDI 1010-6030(94)04008-7

version and ISC were assumed to occur in the excited complex formed between the excited aromatic molecule and the quencher.

The aim of this work was to investigate the processes accompanying the fluorescence quenching of the BA TICT state by inorganic ions in polar solvents. Experimentally determined quantum yields of triplet state formation as a function of the quencher concentration and solvent polarity were analysed in terms of a multistep reaction model. Distinct electron transfer and ISC steps from the singlet and triplet states of the geminal radical pair formed by photoinduced electron transfer were considered. The transient kinetics of quenching of BA were compared with those of anthracene. The effects of solvent relaxation on the transient kinetics of the radical pairs and on the electron transfer recombination rates leading directly to the ground state were studied.

2. Experimental details

BA was synthesized and purified using reported procedures [13]. All solvents were of spectroscopic grade; the quenchers (NaI, LiBr, KSCN, $NaClO_4$ and EtI) were of analytical grade and were used without purification. The fluorescence spectra and their intensities were measured on a Spex Fluorolog fluorometer equipped with an EMI R928 photomultiplier working in the single photon counting mode. Samples were degassed by the freeze–pump–thaw procedure. The shape of the fluorescence spectra remained the same on addition of the quenchers. The relative fluorescence intensities were obtained from integrated fluorescence spectra. Transient absorption measurements were performed by excitation with an XeF excimer laser (351 nm, 25 ns pulse width) or a conventional microsecond discharge flash lamp [10]. In the conventional flash photolysis measurements, Schott bandpass filters (BG12; transmission window, 350–500 nm) were inserted between the flash lamps and the samples to avoid excitation and ionization of the quenchers.

Quantum chemical calculations to predict the triplet–triplet absorption of BA were performed using the open-shell PPP SCF SCI program described previously [14]. Rotation of the anthracenyl moieties about the 9,9′ single bond was simulated by variation of the corresponding resonance integral β.

3. Results

The fluorescence spectra of BA in various solvents have been reported previously [2,6]. The fluorescence spectra of BA in non-polar solvents resemble those of anthracene, but show less vibrational structure and are red shifted by about 1000 cm^{-1}. In solvents of high polarity, a second structureless band is observed at longer wavelength, which is attributed to emission from the TICT state.

The lowest triplet state of BA is the only intermediate observed by nanosecond transient absorption spectroscopy. The spectrum exhibits a single absorption band in the visible region at $\lambda_{max}=430$ nm [9] (Fig. 1). The triplet lifetimes and triplet–triplet absorption spectra of ^{3}BA in polar solvents show little solvent dependence. The absorption spectrum of ^{3}BA, calculated by the PPP SCF SCI method, is the same as that of anthracene (first allowed band at 398 nm, oscillator strength $f=0.6$) when the two anthryl moieties are assumed to be orthogonal to each other, i.e. $\beta_{99'}=0$. Reduction of this angle to 60°, i.e. setting $\beta_{99'}=0.5\beta_0=-1.159$ eV, has little influence on the transition, which is calculated to lie at 425 nm, $f=0.8$. However, a second transition of similar intensity is predicted to appear at much higher wavelength, $\lambda_{max}=765$ nm, $f=0.9$. The absence of any detectable absorption up to 750 nm in the observed spectrum of ^{3}BA in all solvents indicates that the two anthryl moieties are very nearly perpendicular in the relaxed triplet state.

The ISC quantum yields of BA in several solvents were determined by the method of Medinger and Wilkinson [15] (see Section 4). Ethyl iodide was used as a heavy atom perturber. The data collected in Table 1 show that, in polar solvents, where the TICT state of BA is formed, the ISC quantum yields and fluorescence lifetimes are hardly dependent on the solvent polarity, in contrast with the fluorescence quantum yields.

The fluorescence quenching data of BA in acetonitrile, ethanol and propanol are collected in Table 2. The relative quenching efficiencies of the TICT fluorescence of BA by various inorganic anions are similar to those for other aromatic molecules; iodide and thiocyanide ions quench the BA fluorescence more efficiently than

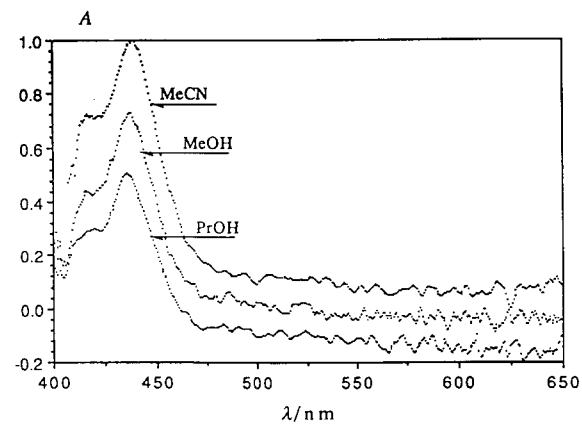

Fig. 1. Triplet–triplet absorption spectra of bianthryl (BA) in acetonitrile, methanol and *n*-propanol, measured approximately 160 ns after 351 nm laser excitation.

Table 1
Intersystem crossing quantum yields and triplet lifetimes of BA in various solvents

Solvent	τ_F (ns)	Φ_F [5]	Φ_{ISC} [a]	τ_T (ms)
MeCN	35 [5]	0.22	0.49±0.01 (7)	0.9±0.12
MeOH		0.33	0.36±0.02 (6)	1.14±0.28
EtOH	33 [5]	0.39	0.40±0.03 (8)	0.8±0.13
PrOH	33 [3]	0.50	0.36±0.004 (6)	0.4±0.08
Hexane	8 [5]	0.55	0.17±0.004 (6)	0.3±0.04

[a] Determined by the method of Medinger and Wilkinson [15] using EtI as a heavy atom quencher. Numbers in parentheses indicate the number of experimental points.

Table 2
Fluorescence quenching of BA by small inorganic anions

Solvent	Anion	ΔG_{et} (eV)	K_{SV} (M^{-1})	k_q (10^9 M^{-1} s^{-1})
MeCN	Br^-	+0.24	11.7±0.2	0.33
	SCN^-	+0.04	101.0±2.0	2.88
	I^-	−0.26	88±1.8	2.51
	ClO_4^-		0.8±0.04	0.02
EtOH	Br^-	+0.5	1.4±0.07	0.044
	SCN^-	+0.1	20.3±0.41	0.63
	I^-	0.0	57.9±1.2	1.81
PrOH	Br^-	+0.5	0.9±0.05	0.028
	SCN^-	+0.1	9.7±0.2	0.303
	I^-	0.0	34.0±0.7	1.06

ΔG_{et} was calculated using the formula

$$-\Delta G_{et} = E_{CT} + [E_{1/2}^{red}(An) - E_{1/2}^{ox}(X^-)]$$

where $E_{1/2}^{red}(An)$ and $E_{1/2}^{ox}(X^-)$ are the half-wave reduction and oxidation potentials of anthracene and of the inorganic anions in the corresponding solvents. The electrochemical data were taken from Refs. [8] and [16].

bromide ions. The solvent dependence is typical for electron transfer quenching; the fluorescence quenching rate constant is higher in acetonitrile than in the less polar solvents ethanol and *n*-propanol with slower dielectric relaxation [2].

In most cases, the fluorescence quenching of BA results in an increase in the triplet quantum yield. However, in some cases, we observe a distinct decrease in the triplet state population. The relative triplet quantum yields of BA as a function of the thiocyanide concentration in acetonitrile and ethanol are presented in Fig. 2. A decrease in the triplet quantum yield of BA is observed in the presence of thiocyanide anions in both solvents. Fig. 2 also contains the results for anthracene (An) in the presence of thiocyanide anions in acetonitrile. Here, contrary to BA, we observe an increase in the triplet quantum yield with increasing quencher concentration; at high quencher concentrations, the ISC quantum yield approaches unity (the ISC quantum yield of anthracene in the absence of quencher is 0.74 [8]).

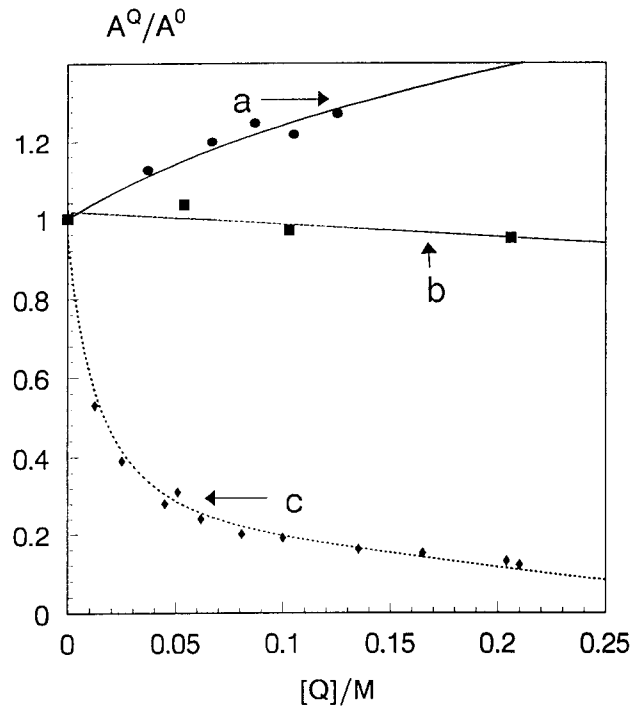

Fig. 2. Dependence of the relative triplet quantum yields of anthracene on the thiocyanide concentration in acetonitrile (a) and of bianthryl (BA) in ethanol (b) and acetonitrile (c). A^Q and A^0 are the initial transient absorbances of the BA triplet in the presence and absence of quencher Q respectively.

4. Discussion

4.1. Kinetic analysis of the reaction scheme

The processes accompanying the fluorescence quenching of the TICT state included in our model are summarized in Scheme 1. In polar solvents, the locally excited state of BA forms the ^{1}TICT state (**1**) with a quantum yield close to unity [2]. ISC of **1** to the nearby ^{3}TICT state (**1′**) and back electron transfer from **1′** populates the BA molecular triplet state ^{3}LE (**4**). The ground state (**0**) is directly recovered by back electron transfer from **1**. We may also consider an alternative route for ISC: the direct charge reversal from the ^{1}TICT state to the ^{3}LE state of BA. For completeness, we include this direct transition between **1** and **4** in Scheme 1, although this process is thought to be unimportant (see below).

Electron transfer between the ^{1}TICT state **1** and the inorganic ion X^- produces the geminal radical pair $^1(BA^-/X)$ in its singlet state (**2**); quenching of the ^{3}TICT state **1′** gives the radical pair $^3(BA^-/X)$ in its triplet state (**2′**). ISC between the states $^1(BA^-/X)$ (**2**) and $^3(BA^-/X)$ (**2′**) is induced by spin–orbit coupling (intraradical spin–orbit coupling (IRSOC) [11,17,18]) and hyperfine interactions between nuclear and electron spins. Back electron transfer from $^1(BA^-/X)$ (**2**) produces the ground state **0**, whereas recombination of

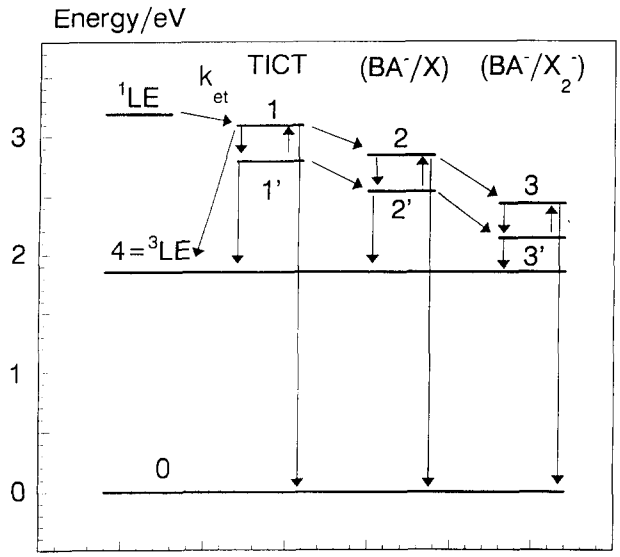

Scheme 1. Key of abbreviations. States: **1**, **1'**, singlet and triplet TICT states of BA; **2**, **2'**, singlet and triplet radical pairs (BA^-/X); **3**, **3'**, singlet and triplet states of complexed radical pairs (BA^-/X_2^-); **4**, molecular triplet state of BA; **0**, ground state of BA. The energies (vertical scale) refer to singlet states (**1**, **2** and **3**). Energy gaps between singlet and triplet states are exaggerated for presentation purposes. The rate constants representing the transitions between the states are identified as k_{XY} (for example the rate constant for the transition from **1** to **1'** is $k_{11'}$). The processes $1 \rightarrow 2$, $2 \rightarrow 3$, $1' \rightarrow 2'$ and $2' \rightarrow 3'$ are bimolecular reactions.

the radical pair in the triplet state $^3(BA^-/X)$ (**2'**) populates the molecular triplet state **4**.

In the presence of excess anion X^-, the radical pairs $^1(BA^-/X)$ and $^3(BA^-/X)$ produce $^1(BA^-/X_2^-)$ (**3**) and $^3(BA^-/X_2^-)$ (**3'**) respectively [10,11,17]. The radical pairs **3** and **3'** have lower energies than those of **2** and **2'**. Our scheme does not include radical separation processes, since free radical ions were not observed.

The overall behaviour of the system depends on the relative magnitudes of the rates of electron transfer, of ISC between the ^{1,3}TICT states and the two types of radical pairs $^1(BA^-/X) \rightleftharpoons {}^3(BA^-/X)$ and $^1(BA^-/X_2^-) \rightleftharpoons {}^3(BA^-/X_2^-)$ and of complex formation $(BA^-/X) + X^- \rightarrow (BA^-/X_2^-)$.

Taking into account the photophysical processes shown in Scheme 1, we obtain the following kinetic equation for the formation of the molecular triplet state of BA

$$\frac{d[4]}{dt} = k_{14}[1] + k_{1'4}[1'] + k_{2'4}[2'] + k_{3'4}[3'] \quad (1)$$

Under continuous excitation, the steady state approximation (Eq. (2)) is satisfied

$$\frac{d[i]}{dt} = 0, \text{ for } i = 1', 2, 2', 3, 3' \quad (2)$$

From Eq. (2), the following equations for the populations of the transients **1'**, **2**, **2'**, **3** and **3'** can be obtained

$$[1'] = \frac{k_{11'}[1]}{k_{1'4} + k_{1'1} + k_{1'2'}[Q]} \quad (3)$$

$$[3] = \frac{k_{23}[Q][2] + k_{3'3}[3']}{k_{30} + k_{33'}} \quad (4)$$

$$[3'] = \frac{k_{2'3'}[Q][2'] + k_{33'}[3]}{k_{3'3} + k_{3'4}} \quad (5)$$

$$[2] = \frac{k_{12}[Q][1] + k_{2'2}[2']}{k_{20} + k_{22'} + k_{23}[Q]} \quad (6)$$

$$[2'] = \frac{k_{1'2'}[Q][1'] + k_{22'}[2]}{k_{2'2} + k_{2'4} + k_{2'3'}[Q]} \quad (7)$$

Introducing Eqs. (3) and (6) into Eq. (7), we obtain the following equation for the population of **2'**

$$[2'] = \frac{k_{1'2'}[Q][k_{11'}/k_{1'4} + k_{1'1} + k_{1'2}[Q])] + \phi_2{}^Q k_{12}[Q]}{k_{2'4} + k_{2'3'}[Q] + k_{2'2}(1 - \phi_2{}^Q)} \quad [1] \quad (8)$$

where $\phi_2{}^Q = k_{22'}/(k_{20} + k_{22'} + k_{23}[Q])$ represents the efficiency of the spin inversion $^1(BA^-/X) \rightarrow {}^3(BA^-/X)$.

Similar equations can be derived for the steady state concentrations of **2**, **3** and **3'**. The expressions for the populations of these states are functions of [**1**]. The final kinetic equation for the formation of the molecular triplet state of BA as a function of [**1**] has the following form

$$\frac{d[4]}{dt} = \left(k_{14} + \frac{k_{1'4}k_{11'}}{k_{1'4} + k_{1'1} + k_{1'2'}[Q]} + \phi_3 \frac{k_{3'4}k_{23}[Q]k_{12}[Q]\phi_2{}^Q}{[k_{3'4} + k_{3'3}{}^*(1 - \phi_3)]k_{22'}} + \left\{ k_{2'4} + \frac{k_{3'4}k_{2'3'}[Q]}{k_{3'4} + k_{3'3}(1 - \phi_3)} + \phi_3 \frac{k_{3'4}k_{23}[Q]k_{2'2}\phi_2{}^Q}{[k_{3'4} + (1 - \phi_3)]k_{22'}} \right\} \times \frac{(k_{1'2'}[Q]k_{11'})/(k_{1'4} + k_{1'1} + k_{1'2'}[Q]) + \phi_2{}^Q k_{12}[Q]}{k_{2'4} + k_{2'3'}[Q] + k_{2'2}(1 - \phi_2{}^Q)} \right) \times [1] = B^Q[1] \quad (9)$$

where $\phi_3 = k_{33'}/(k_{30} + k_{33'})$ defines the efficiency of the spin inversion $^1(BA^-/X_2^-) \rightarrow {}^3(BA^-/X_2^-)$.

In the absence of quencher Q, Eq. (9) reduces to

$$\frac{d[4]}{dt} = \left(k_{14} + \frac{k_{1'4}k_{11'}}{k_{1'4} + k_{1'1}} \right)[1] = B^0[1] \quad (10)$$

Integration of Eq. (9) yields

$$[4]^Q(t) = c \frac{B^Q}{1/\tau_F{}^0 + k_{12}[Q]} [1 - \exp(-t/\tau_F)] \quad (11)$$

where $1/\tau_F = 1/\tau_F{}^0 + k_{12}[Q]$; $\tau_F{}^0$ and τ_F are the lifetimes of the TICT fluorescence of BA in the absence and presence of quencher respectively and c is a factor which depends on the intensity of the exciting light, the sample absorbance at the excitation wavelength and geometrical factors. The factor c is kept constant in all experiments.

The time scales of the fluorescence and triplet decays for aromatic hydrocarbons are very different. The triplet population grows in parallel with the fluorescence decay and decays several orders of magnitude more slowly than the fluorescence. When the fluorescence decay is completed, the population of the triplet state reaches its maximum value. This point is taken as time zero ($t=0$) for the triplet state decay. This is a good approximation on the time scale of the triplet state decay of aromatic molecules in oxygen-free polar solvents. Accordingly, the initial population of the triplet state is given by

$$[\mathbf{4}]_{t=0}{}^{Q}=c\,\frac{B^{Q}}{1/\tau_F{}^{0}+k_{12}[Q]} \tag{12}$$

The relative initial triplet population ($[\mathbf{4}]_{t=0}{}^{Q}/[\mathbf{4}]_{t=0}{}^{0}$) may be easily derived from Eqs. (9)–(12) and has the form

$$\frac{[\mathbf{4}]^{Q}}{[\mathbf{4}]^{0}}=\frac{B^{Q}}{B^{0}}\,\frac{1}{1+K_{SV}[Q]} \tag{13}$$

Using the Stern–Volmer relation (Eq. (14)), which holds for the fluorescence quenching of the ^{1}TICT state of BA by inorganic anions

$$K_{SV}[Q]=k_{12}\tau_F{}^{0}[Q]=\frac{\phi_F{}^{0}}{\phi_F{}^{Q}}-1 \tag{14}$$

we arrive at the following relation

$$\frac{[\mathbf{4}]^{Q}\Phi_F{}^{0}}{[\mathbf{4}]^{0}\Phi_F{}^{Q}}=\frac{B^{Q}}{B^{0}} \tag{15}$$

Eq. (15) may be expressed in more explicit form by introducing B^{Q} and B^{0} from Eqs. (9) and (10), the Stern–Volmer relation (Eq. (14)) and the definition of the ISC quantum yield of BA in the absence of quencher (Eq. (16))

$$\Phi_{ISC}=\left(k_{14}+\frac{k_{1'4}k_{11'}}{k_{1'4}+k_{1'1}}\right)\tau_F{}^{0} \tag{16}$$

We obtain

$$\frac{A^{Q}\Phi_F{}^{0}}{A^{0}\Phi_F{}^{Q}}-L([Q])=\frac{1}{\Phi_{ISC}}\,b([Q])\left(\frac{\Phi_F{}^{0}}{\Phi_F{}^{Q}}-1\right) \tag{17}$$

where A^{Q} and A^{0} are the initial absorbances of the molecular triplet state in the presence and absence of quencher respectively and the functions $L([Q])$ and $b([Q])$ are given by

$$L([Q])=\frac{k_{1'4}+k_{1'1}}{k_{1'4}+k_{1'1}+k_{1'2'}[Q]}\times\left[\frac{k_{14}(k_{1'4}+k_{1'1}+k_{1'2'}[Q])+k_{1'4}k_{11'}}{k_{14}(k_{1'4}+k_{1'1})+k_{1'4}k_{11'}}+\frac{k_{1'2'}[Q]k_{11'}}{k_{14}(k_{1'4}+k_{1'1})+k_{1'4}k_{11'}}R([Q])\right] \tag{17a}$$

$$b([Q])=\left\{\frac{\phi_3k_{3'4}k_{23}[Q]}{[k_{3'4}+k_{3'3}(1-\phi_3)]k_{22'}}+R([Q])\right\}\phi_2{}^{Q} \tag{17b}$$

where $R([Q])$ is defined as

$$R([Q])=\{k_{2'4}+[k_{3'4}/(k_{3'4}+k_{3'3}(1-\phi_3))][k_{2'3'}[Q]+\phi_3(\phi_2{}^{Q}k_{23}[Q]k_{2'2}/k_{22'})]\}/\{[k_{2'4}+k_{2'3'}[Q]+k_{2'2}(1-\phi_2{}^{Q})]\} \tag{17c}$$

Eq. (17) has a form similar to the equation derived by Medinger and Wilkinson [15]. We recover the Medinger–Wilkinson equation when $L([Q])=1$ and $b([Q])=1$. The Medinger–Wilkinson equation has been frequently applied to estimate the ISC quantum yields under the assumption that appropriately chosen quenchers containing heavy atoms accelerate ISC from the excited singlet state without influencing the internal conversion rate. The derivation presented above suggests that, in some cases, the Medinger–Wilkinson method may be generalized. We show below that $L([Q])$ and $b([Q])$ are indeed close to unity for the quenching of anthracene.

Medinger–Wilkinson plots for anthracene in the presence of I^-, Br^-, SCN^- and ethyl iodide give superimposable straight lines. The function $b([Q])$ is constant and equal to unity in these four cases. Thiocyanide ions are also effective as heavy atom perturbers as can be seen in Fig. 3(a). This shows that, for electron transfer quenching of anthracene fluorescence by inorganic ions, the recombination reactions favour the formation of the molecular triplet. Direct recombination of radical pairs to the ground state seems to play a minor role.

The first function $L([Q])$ of Eq. (17) can be approximated by unity, since the rate coefficient $k_{1'4}$ is expected to be very large. In order to prove this assumption, we used 4,4′-dimethoxystilbene (DMS) as an electron donor to show that the lifetime of the ^{3}TICT (**1′**) state is very short. The donating property of DMS is similar to that of SCN^- anions in acetonitrile. The radical cation of DMS possesses a large absorption coefficient at about 530 nm. This compound was used by Gould et al. [19] as a cosensitizer in transient absorption measurements to monitor the fluorescence quenching of 9,10-dicyanoanthracene in acetonitrile. In systems containing BA and DMS in acetonitrile, the absorption bands of the radical cation of DMS were readily observed by flash photolysis, but after the addition of ethyl iodide in amounts sufficiently large to quench the BA fluorescence completely, the absorption bands of DMS^+ were absent. Since ethyl iodide is expected to accelerate the transition of the singlet TICT state of BA to its triplet TICT state, the absence of

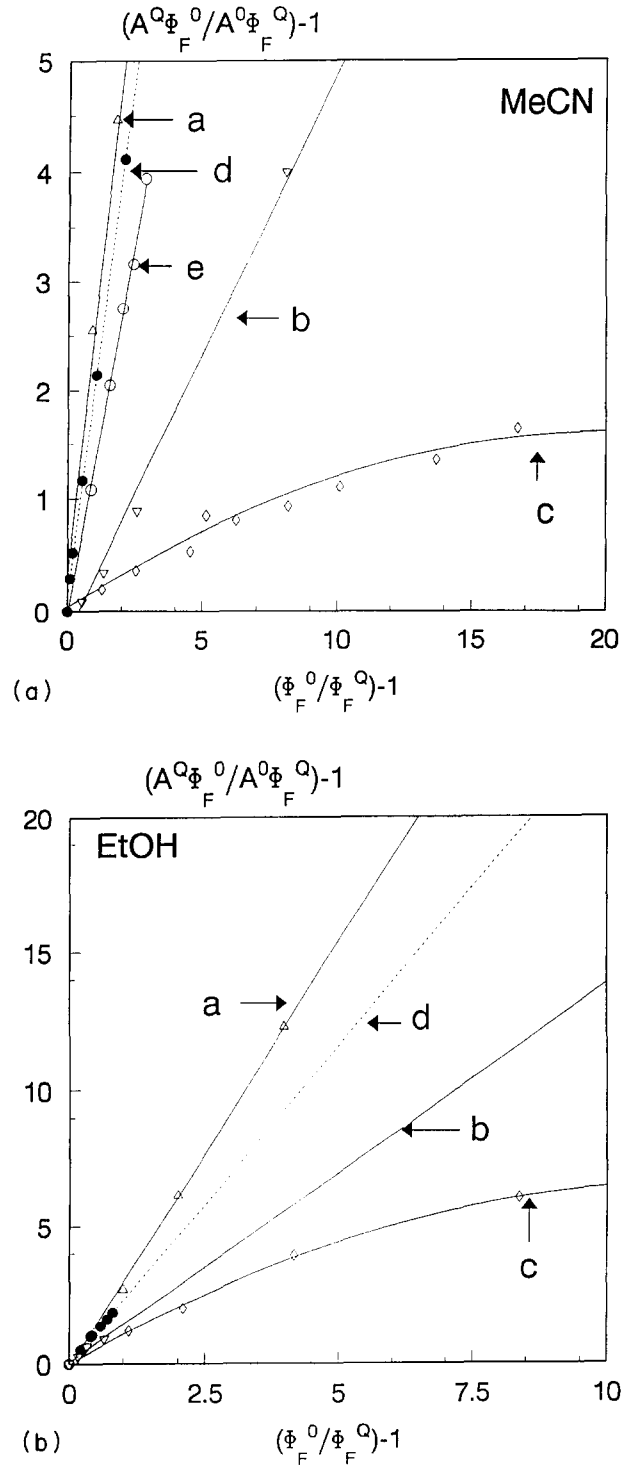

Fig. 3. (a) Dependence of the product of the relative triplet and fluorescence quantum yields on the relative fluorescence quantum yields of bianthryl (BA) in the presence of the quenchers I^- (a), Br^- (b), SCN^- (c) and EtI (d) and of anthracene with SCN^- (e) in acetonitrile. (b) The same as (a) for ethanol solutions.

the DMS^+ bands indicates that quenching of the ^{3}TICT state is negligible due to its short lifetime; the quenching of the singlet and triplet TICT states of BA by DMS should proceed with almost the same rate.

Alternatively, when the direct ISC $^1TICT \rightarrow {}^3LE$ is the dominant route for the population of the molecular triplet state, i.e. when $k_{11'} \ll k_{14'}$, the function $L([Q]) = 1$ at all concentrations.

When $L([Q]) = 1$, Eq. (17) reduces to a form suitable for analysis

$$\left(\frac{A^Q\Phi_F^0}{A^0\Phi_F^Q} - 1\right)\Phi_{ISC} \Big/ \left(\frac{\Phi_F^0}{\Phi_F^Q} - 1\right) = b([Q]) \qquad (18)$$

Here we can distinguish three concentration regions for the function $b([Q])$, which for our purposes is defined by Eqs. (17b) and (17c): low, moderate and large quencher concentrations. At large quencher concentrations, the practical utility of Eq. (17) is limited, since the function $L([Q])$ may differ from unity. Under such circumstances, the Medinger–Wilkinson type of analysis cannot be applied.

Figs. 3(a) and 3(b) show the dependence of the product of the relative triplet and fluorescence quantum yields on the relative fluorescence quantum yields (Medinger–Wilkinson plots) for BA in acetonitrile and ethanol. For comparison, the data for anthracene and SCN^- in acetonitrile are also shown.

Most instructive are the results obtained at low concentrations when complex formation becomes unimportant and the approximation $L([Q]) = 1$ should hold well. The limiting value of the function $b([Q])$ for quencher concentrations approaching zero is equal to

$$b([Q] \longrightarrow 0) = k_{2'4}\phi_2^0 / [k_{2'4} = k_{2'2}(1 - \phi_2^0)] \qquad (19)$$

This result is exact. Experimental values of the constant $b([Q] \rightarrow 0)$ can therefore be obtained from the initial slopes of the Medinger–Wilkinson plots (see Fig. 3 and Table 3), since Φ_{ISC} is known. These results will be discussed in Section 4.4.

When spin inversion in the complexed radical pair (BA^-/X_2^-) $(k_{3'3})$ is slower than back electron transfer to the triplet state $(k_{3'4})$, Eq. (17b) simplifies as follows

Table 3
Initial slopes of Medinger–Wilkinson plots (Eq. (18))

Solvent	Φ_{ISC}	Quencher	$b'^{-1}([Q] \rightarrow 0)$ [a]
MeCN	0.49 ± 0.01 [b]	EtI	0.49 ± 0.01 [b]
		I^-	0.44 ± 0.005
		Br^-	1.67 ± 0.16
		SCN^-	5.96 ± 0.66
EtOH	0.40 ± 0.3 [b]	EtI	0.40 ± 0.03 [b]
		I^-	0.33 ± 0.04
		Br^-	0.47 ± 0.1
		SCN^-	0.88 ± 0.04

[a] The parameters $b'([Q] \rightarrow 0)$ are the initial slopes of the plots shown in Fig. 3 $(b'([Q] \rightarrow 0) = b([Q] \rightarrow 0)/\Phi_{ISC})$. Definitions of $b([Q] \rightarrow 0)$ are given in Eqs. (19) and (27).

[b] From Table 1.

$$b([Q]) = \left[\phi_3 \frac{k_{23}[Q]}{k_{22'}} + \frac{k_{2'4} + k_{2'3'}[Q] + \phi_3 k_{23}[Q](k_{2'2}/k_{22'})\phi_2^Q}{k_{2'4} + k_{2'3'}[Q] + k_{2'2}(1-\phi_2^Q)} \right] \phi_2^Q \quad (20)$$

Moreover, when

$$k_{2'2}(1-\phi_2^Q) \ll k_{2'4} + k_{2'3'}[Q]$$

which holds in the presence of high concentrations of inorganic anions, Eq. (20) reduces to

$$b([Q]) = (\phi_3 k_{23}[Q] + k_{22'})/(k_{20} + k_{22'} + k_{23}[Q]) \quad (21)$$

When the interconversion rate between the singlet and triplet states of the radical pair (BA^-/X_2^-) is negligible, $\phi_3 \approx 0$ for $X_2^- = (SCN)_2^-$, the following inequality holds at intermediate quencher concentrations

$$\phi_3 k_{23}[Q] \ll k_{22'}$$

From Eq. (21), we arrive at

$$1/b([Q]) = 1 + k_{20}/k_{22'} + k_{23}[Q]/k_{22'} \quad (22)$$

For the thiocyanide ions, the function $b([Q])$ is less than unity and clearly concentration dependent (Figs. 3(a) and 3(b)). The relationship $b([Q])^{-1}$ vs. [Q] is shown in Fig. 4 for the two solvents acetonitrile and ethanol. The linearity predicted by Eq. (22) holds within

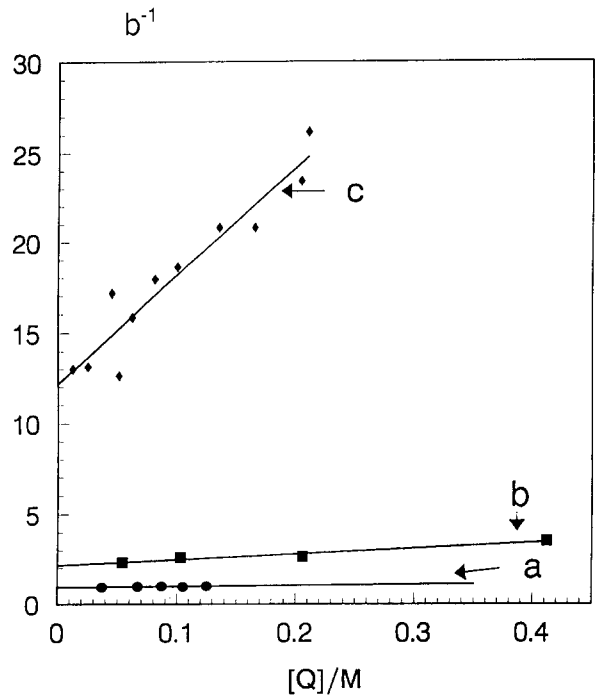

Fig. 4. Dependence of the inverse of parameter b (for details see text) on the quencher concentration for anthracene and SCN^- in acetonitrile (a), bianthryl (BA) and SCN^- in ethanol (b) and BA and SCN^- in acetonitrile (c).

experimental accuracy. Below, we show that the parameters obtained from the intercepts and slopes of these plots for the two solvents acetonitrile and ethanol are reasonable.

Analysis of the data for the systems containing thiocyanide anions in acetonitrile and ethanol solutions yields the ratios $k_{20}/k_{22'}$ and $k_{23}/k_{22'}$ given in Table 4. Since $k_{22'}$ should be largely independent of the solvent, we were able to calculate the ratios of the back electron transfer (k_{20}) and complex formation (k_{23}) rate constants in both solvents. The results show that the change in solvent from acetonitrile to ethanol reduces the complex formation rate more strongly than the back electron transfer rate.

The ratio of the back electron transfer rate constants (k_{20}) for BA in the presence of SCN^- in acetonitrile and ethanol (see Table 4) seems reasonable in view of electron transfer theory, but the corresponding ratio of the complex formation rate constants (k_{23}) is very different from the ratio of the viscosity coefficients of the two solvents. The latter case needs further discussion.

Let us consider the process of complex formation from the primary radical pair $(BA^-/X) + X^- \rightarrow (BA^-/X_2^-)$. This process is controlled by diffusion and its efficiency depends on the lifetime of the radical pair. The lifetime of the radical pair is determined by the rate constant of back electron transfer (k_{20}), which is smaller in ethanol than in acetonitrile by a factor of ten. This large difference in the lifetime arises from the time dependence of the rate coefficients for diffusion-controlled reactions. For our purposes, the reaction rate coefficient can be evaluated using an equation derived by Keizer [20]

$$k_{23} = \frac{4\pi NDRk^0 C(R)}{4\pi NDRC(R) + k^0} \quad (23)$$

where D is the sum of the diffusion coefficients of the reactants, R is the distance as the reaction occurs, k^0 is the reaction rate constant at the distance R and N is Avogadro's constant. The parameter $C(R)$ is given by the equation

$$C(R) = \exp(R\alpha^{1/2})$$

where

$$\alpha = (\tau^{-1} + k_{23}[Q])/D_A = 2(\tau^{-1} + k_{23}[Q])/D \quad (23a)$$

D_A is the diffusion coefficient of the radical pair, assumed to be one-half of the mutual diffusion coefficient D, and τ is the lifetime of the radical pair. When $k^0 \gg 4\pi NDRC(R)$ and at low quencher concentrations, Eq. (23) reduces to

$$k_{23} = 4\pi NDRC(R) = 4\pi NDR \exp\left[R\left(\frac{2}{\pi D}\right)^{1/2} \right] \quad (24)$$

Table 4
Estimated deactivation parameters for the systems BA^-/SCN in acetonitrile and ethanol

Parameter	MeCN	EtOH	Method of estimation
$k_{20}/k_{22'}$	11.16±1.41	1.16±0.15	Eq. (22)
$k_{23}/k_{22'}$	60.2±6.4	3.19±0.54	Eq. (22)
$k_{2'4}$ (10^{10} s^{-1})	3.16 ($\Delta G = -1.28$ eV)	4.36 ($\Delta G = -1.34$ eV)	Eqs. (25) and (26)
k_{20} (10^8 s^{-1})	8.51 ($\Delta G = -3.13$ eV)	1.21 ($\Delta G = -3.19$ eV)	Eqs. (25) and (26)
k_{20} (10^{10} s^{-1})	13.1	1.31	Eq. (23)
$k_{2'2}$ (10^9 s^{-1})	6.0	5.3	Eq. (28)
$k_{22'}$ (10^{10} s^{-1})	1.8	1.59	$k_{22'} = 3k_{2'2}$
$k_{22'}$ (10^{10} s^{-1})	1.13	1.13	Eq. (24)
k_{23} (10^{10} M^{-1} s^{-1})	68.0	3.60	Eq. (22)

When thiocyanide anions are used as quenchers, the ratio $k_{23}^{MeCN}/k_{23}^{EtOH}$ is equal to 18.87. From the data collected in Table 4, we find that the lifetime of the $^1(BA^-/SCN)$ pair in acetonitrile is approximately five times shorter than that in ethanol. Assuming that the ratio of the mutual diffusion coefficients in acetonitrile and ethanol is equal to two, we can calculate the lifetimes of the above-mentioned radical pairs. Setting the same encounter distances for complex formation in acetonitrile and ethanol ($R_{MeCN} = R_{EtOH} = 550$ pm), and $D_{MeCN} = 2D_{EtOH} = 4 \times 10^{-5}$ cm^2 s^{-1}, we obtain $\tau_{MeCN} = k_{20}^{-1}$ (in MeCN) = 4.1 ps. Similarly, $\tau_{EtOH} = (k_{20}^{EtOH} + k_{22'})^{-1} = 41$ ps. Setting $k_{20}^{EtOH}/k_{22'}^{EtOH} = 1.16$ (Table 4), we obtain $k_{20} = 1.31 \times 10^{10}$ s^{-1} and $k_{22'} = 1.13 \times 10^{10}$ s^{-1}.

4.2. Electron transfer rates

For the probability of electron transfer between donor and acceptor molecules, separated by a distance r, we use the Onuchic formula [21]

$$k_{et}(r) = \sum_{m=0}^{\infty} \frac{(2\pi/\hbar)V(r, m)^2[4\pi\lambda(r)kT]^{-1/2}}{1 + (4\pi/\hbar)V(r, m)^2\tau_L/\lambda(r)} \times \exp\left\{ - \frac{[\Delta G + m\hbar\Omega + \lambda(r)]^2}{4\lambda(r)kT} \right\} \quad (25)$$

where

$$V(r, m)^2 = V(r)^2 \exp(-S)S^m/m!, \text{ with } S = \lambda_{in}/\hbar\Omega$$

In Eq. (25), ΔG is the free enthalpy change between reactants and products and $\lambda(r)$ and λ_{in} are the solvent and internal reorganization energies respectively. $V(r)$ is the matrix element of the electronic coupling. The longitudinal relaxation time τ_L can be evaluated from the Froehlich formula $\tau_L = (\epsilon_\infty/\epsilon_S)\tau_D$, where ϵ_S and ϵ_∞ are the static and optical dielectric permittivities of the solvent respectively and τ_D is the Debye relaxation time. The solvent reorganization energy $\lambda(r)$ may be approximated by the Marcus formula [22] which has the form

$$\lambda(r) = Ne^2(1/2a_1 + 1/2a_2 - 1/r)(1/\epsilon_\infty - 1/\epsilon_S)/4\pi\epsilon_0 \quad (26)$$

where a_1 and a_2 are the radii of the reactants, e is the electron charge and $\epsilon_\infty = n^2$ (n is the refractive index). For the electronic matrix element $V(r)$, we use the standard formula

$$V(r) = V(a) \exp[-\alpha(r-a)/2]]$$

where the scaling factor α describes the distance dependence of $V(r)$ and a is the distance of closest approach of the reactants.

Fig. 5 presents the results of model calculations of the dependence of the electron transfer rate constants on ΔG calculated using Eq. (25) and the parameters collected in Table 5. In the inverted Marcus region,

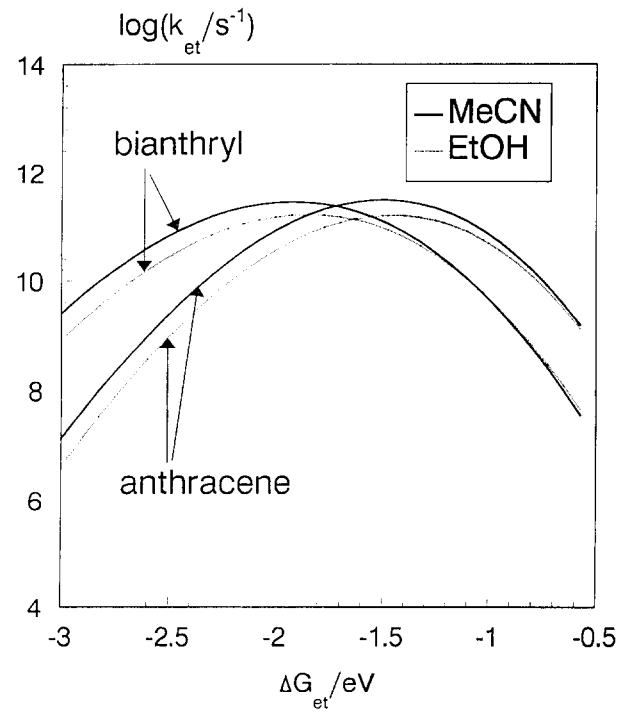

Fig. 5. Dependence of $\log k_{et}$ vs. ΔG calculated using Eqs. (25) and (26), with the parameters collected in Table 5. Encounter distances $a_0 = 600$ pm and 900 pm represent the situations for anthracene and bianthryl respectively.

Table 5
Parameters used in model calculations of the dependence of k_{et} on ΔG_{et}

Parameter	MeCN	EtOH
a_1 (pm)	220	220
a_2 (pm)	420	420
a_3 (pm)	600 (An) or 900 (BA)	600 (An) or 900 (BA)
ϵ_S	37.5	24.5
n	1.3441	1.3614
τ_L (ps)	0.5	9.6
$\hbar\Omega(a_0)$ (eV)	0.005	0.005
S	1	1
$\hbar\Omega$ (eV)	0.15	0.15
α (pm^{-1})	0.01	0.01
T (K)	293	293

Description of parameters: a_1, a_2, radii of the reactants (X and BA^- radicals); a_0, encounter distance; ϵ_S, dielectric constant of the solvent; n, refractive index of the solvent; τ_L, longitudinal relaxation time of the solvent; S, displacement parameter; $\hbar\Omega$, energy of internal vibration; α, scaling factor.

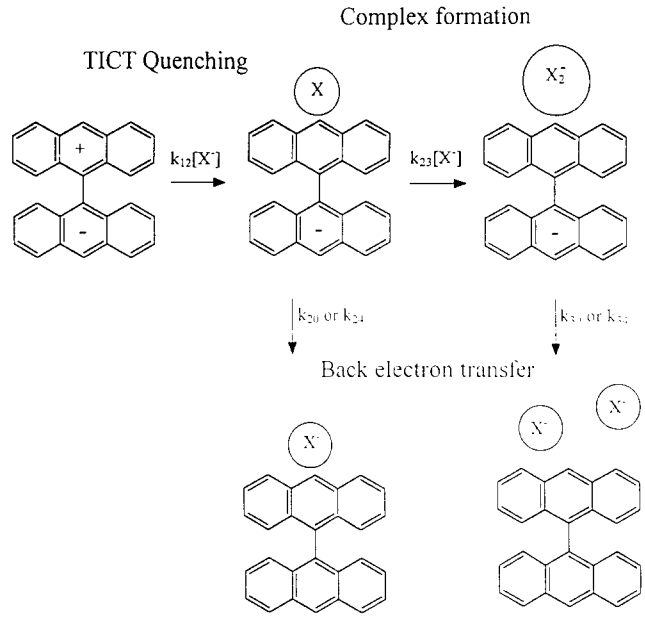

Scheme 2.

The electron transfer rate constants (k_{20}) are smaller in ethanol than in acetonitrile (see Fig. 5 and Table 5), which explains the higher efficiency of molecular triplet production for BA in the presence of thiocyanide anions in ethanol than in acetonitrile.

The different quenching behaviour of BA and anthracene may be explained in the following way. The primary electron transfer process, which results in fluorescence quenching, proceeds at a certain distance. Let us assume that the encounter distance for both systems is 600 pm, obtained from previous work [23,24]. The anion is attracted to the vicinity of the positively charged anthracene moiety of the BA molecule prior to the primary electron transfer process. This geometrical situation remains intact on the time scale of the back electron transfer processes (Scheme 2). Thus the back electron transfer reactions which populate the ground and molecular triplet states occur at different distances for anthracene and BA. This is connected with the different solvent reorganization energies of the two systems. The solvent reorganization energy in BA-containing systems is approximately 1.3 times larger than in those containing anthracene. The larger solvent reorganization energy in the BA systems makes the Marcus parabola broader and shifted to more negative values of ΔG. An enhancement of the internal reorganization energy in the BA radical anion compared with that in anthracene, due to the flexibility of BA^-, cannot be ruled out, although we assume that this effect is not large.

Comparing the polarity of acetonitrile and ethanol and the charge distributions in the reactants and products one should expect small solvent effects on the energy gaps between pairs of states BA^-/X–BA/X^- and BA^-/X_2^-–$Ba/2X^-$. In the present evaluations of the rate constants $k_{2'4}$ and $k_{3'4}$ and also k_{20} and k_{30} the energy gaps derived from the electrochemical and spectral data [8,16] have been used.

The redox potentials of (X/X^-) in water are 1.44, 1.64 and 2.04 V [16], while those for ($X_2^-/2X^-$) are 1.03 [25], 1.31 [26] and 1.63 V [25], vs. a saturated hydrogen electrode (SHE) for X≡I, SCN and Br respectively. Electron transfer theory predicts an increase in the back electron transfer rate constants with increasing ΔG for the inverted Marcus region (see Fig. 5). Moreover, the back electron transfer in $^1(BA^-/X_2^-)$ is accompanied by a larger internal reorganization energy, λ_{in}, compared with that in (BA^-/X) which additionally increases k_{30}. Hence the back electron transfer rate constants k_{30} are always higher than k_{20}.

It was pointed out by Linschitz and coworkers [11] that the radicals X_2^- in their $^2\Sigma$ states are expected to be less efficient heavy atom perturbers than the radicals X in their ^2P or $^2\Pi$ states. The ISC rate constants in the complexed radical pairs are therefore expected to be much smaller than in the primary radical pairs [10,11]. On the other hand, the rate constants of the back electron transfer to the ground state increase on complex formation which decreases the energy gap. Hence the efficiency of triplet formation in complexed radical pairs, ϕ_3, is negligible.

The back electron transfer rate constants from the complexed radical pair to the triplet state ($k_{3'4}$) should also be larger than the spin inversion rate constant ($k_{3'3}$) because the free energy change associated with the process **3**→**4** is in the range from −0.58 to −1.04 eV. For this ΔG range, the back electron transfer rate constant is estimated to be greater than 1×10^{10} s^{-1} [10].

For the (An^-/X) radical pair in the singlet state, the back electron transfer process to the ground state

(k_{20}) should be much slower than spin inversion to the triplet radical pair followed by back electron transfer to the triplet state ($k_{2'4}$) in both solvents. This explains the high efficiency of production of triplet anthracene.

4.3. Mechanism of ISC in the TICT state of BA

The betraying feature of TICT excited states is their "anomalous" emission [27]. Therefore the vast majority of photophysical studies concerned with the TICT phenomenon have concentrated on emission studies; singlet–triplet ISC from TICT excited states has received relatively little attention [28]. The data given in Table 1 provide rate constants for spontaneous ISC of BA in various solvents via the relation $k_{ISC} = \Phi_{ISC}/\tau_F^0$. The radical change in the electronic structure of the lowest excited state of BA associated with a change in solvent from hexane, where a local excitation of one of the anthracenyl moieties (^{1}LE) provides an adequate description, to acetonitrile, where the highly polar ^{1}TICT state **1** (Scheme 1) is formed rapidly after excitation [1–6], is accompanied by a surprisingly moderate change in k_{ISC} from 2.1×10^7 s^{-1} (hexane) to 1.4×10^7 s^{-1} (acetonitrile). In the series of polar solvents, k_{ISC} seems to be largely independent of polarity.

The ^{1}TICT state should be nearly degenerate with a triplet state of the same electronic structure, ^{3}TICT, since the two unpaired electrons are spatially separated on the two anthracenyl moieties and the corresponding exchange integrals will be very small. Therefore we might have expected very rapid ISC from the ^{1}TICT state to the ^{3}TICT state of BA, followed by relaxation to the lowest triplet state which corresponds to a locally excited state, ^{3}LE. However, the one-electron spin–orbit coupling operator yields a non-vanishing coupling element only between TICT and LE states, a transition associated with the transfer of an electron between two presumably orthogonal chromophore units [29]. Spin–orbit coupling between the singlet and triplet charge transfer states vanishes, since the orbital character does not change [28f]. The situation is similar to the well-known $n\pi^*$–$\pi\pi^*$ coupling scheme in aromatic ketones. Therefore we might expect that ISC from the ^{1}TICT state of BA occurs predominantly by charge recombination to form the lowest triplet state ^{3}LE. However, the insensitivity of the ISC rate constant to the solvent polarity (Table 1) argues against this notion. The ISC rate constant k_{14} should increase with decreasing solvent polarity as predicted by Marcus theory. On the other hand, the energy gap between the singlet and triplet TICT states is expected to be very small and solvent independent. Recently, Herbich and Kapturkiewicz [30] have provided evidence for the involvement of the ^{3}TICT state as an intermediate in ISC from the ^{1}TICT state to the ^{3}LE state of 4-(9-anthryl)-*N*,*N*-dimethylaniline (A-DMA) and related anthryl derivatives. The non-radiative decay of the ^{1}TICT state of A-DMA was found to be independent of solvent polarity when the TICT fluorescence band positions were higher than 2 eV, i.e. higher than the energy of the lowest triplet state.

For the sake of argument, we have also analysed Scheme 1 assuming that all ISC processes in the TICT states and the radical pairs are slow. Then the direct charge reversal processes **2** → **4** and **3** → **4** would solely be responsible for ISC in the presence of quenchers. Such a model leads to serious inconsistencies with the observed data.

4.4. Heavy atom effect

Table 3 contains the experimental values of the parameter $b([Q]\rightarrow 0)$ defined by Eqs. (18) and (19). For the quenchers containing iodine (ethyl iodide or I^-), the values of these quantities are comparable, but we observe significant solvent effects with the bromide and thiocyanide ions as quenchers.

Eq. (19) may be presented in another form

$$b([Q]\longrightarrow 0) = \frac{k_{22'}[k_{2'4}/(k_{2'4}+k_{2'2})]}{k_{20}+k_{22'}[k_{2'4}/(k_{2'4}+k_{2'2})]} \qquad (27)$$

For $k_{2'4} \gg k_{2'2}$ (weak heavy atom perturber or very efficient back electron transfer to the molecular triplet state), Eq. (27) reduces to

$$b([Q]\longrightarrow 0) = \frac{k_{22'}}{k_{20}+k_{22'}}$$

Under such conditions, the heavy atom effect should be clearly observed.

In the opposite case, when $k_{2'4} \ll k_{2'2}$

$$b([Q]\longrightarrow 0) = \frac{k_{2'4}K}{k_{20}+k_{2'4}K}$$

where $K = k_{22'}/k_{2'2} = 3$, due to spin statistics, and the heavy atom effect is less important. Intermediate situations ($k_{2'2} \approx k_{2'4}$) are also possible.

When $b([Q]\rightarrow 0) = 1$, i.e. $k_{20} \ll k_{22'}$, as in the case of anthracene systems, the triplet state is populated with an efficiency equal to unity when the fluorescence quenching is complete. With heavy atom quenchers containing iodine, it seems that the inequality $k_{20} \ll k_{22'}$ is also fulfilled for BA. In the systems which contain weaker heavy atoms, such as Br or S in SCN radicals, k_{20} appears to be comparable with the spin inversion rate constant $k_{22'}$, which makes the production of the triplet state less effective than in iodine-containing systems.

The values of $b([Q]\rightarrow 0)$ defined by Eq. (27) allow us to determine the values of the spin inversion rate constant $k_{2'2}$ in the case of the thiocyanide- and bromide-containing systems. From Eq. (27), we obtain

$$\frac{(b^{-1}-1)^{SCN}}{(b^{-1}-1)^{Br}} = \frac{k_{20}^{SCN}k_{2'4}^{Br}}{k_{20}^{Br}k_{2'4}^{SCN}} \times \frac{k_{22'}^{Br}}{k_{22'}^{SCN}} \times \frac{(k_{2'4}+k_{2'2})^{SCN}}{(k_{2'4}+k_{2'2}^{Br})} \quad (28)$$

Let us assume that [31]

$$\frac{(k_{20}^{SCN}k_{2'4}^{Br})}{(k_{20}^{Br}k_{2'4}^{SCN})} = 1 \text{ and } \frac{k_{22'}^{Br}}{k_{22'}^{SCN}} = \frac{\xi^2(Br)}{\xi^2(S)} = 41.5$$

Taking $k_{2'4}$ equal to 3.16×10^{10} and 4.36×10^{10} s^{-1}, the values obtained from the model calculations in acetonitrile and ethanol respectively, we find that the rate constants $k_{2'2}$ in the presence of SCN are equal to 0.60×10^{10} and 0.53×10^{10} s^{-1} in acetonitrile and ethanol respectively. This is in reasonable agreement with our previous assumption that the heavy atom effect is solvent independent, as well as with our previous estimate based on an analysis of the transient effects.

One discrepancy emerges from these estimates. The back electron transfer rate constants k_{20} for the systems (BA^-/SCN) in acetonitrile and ethanol are calculated by the Onuchic formula (Eqs. (25) and (26), with $a_0 = 900$ pm, $\Delta G = -3.13$ and -3.19 eV) as $k_{20} = 8.5\times10^8$ and 1.2×10^8 s^{-1} (Table 5) in acetonitrile and ethanol respectively. Thus the calculated back electron transfer rate to the ground state is too slow to compete with the ISC process ($k_{22'} = 1.8\times10^{10}$ s^{-1} and 1.59×10^{10} s^{-1} in acetonitrile and ethanol respectively). It appears that the absolute values of k_{et} are underestimated by the model used.

5. Conclusions

An equation for the triplet quantum yields of aromatic molecules in the presence of electron transfer quenchers has been derived. Under appropriate limiting conditions, it takes the same form as the well-known Medinger–Wilkinson equation which describes the triplet quantum yield dependence on heavy atom perturbers for aromatic molecules. Different physical situations have been considered. In particular, we found that the simple form of the Medinger–Wilkinson equation may be applicable for the determination of the ISC quantum yields when the electron transfer quenchers contain heavy atoms.

When the radical pairs formed by electron transfer fluorescence quenching contain an atom of moderate spin–orbit coupling, such as a sulphur atom in the SCN radical, an extended equation must be used for the analysis of the experimental data to yield self-consistent estimates of the kinetic parameters. The present model uses the concept of IRSOC. The efficiency of ISC induced by electron transfer fluorescence quenching is higher for anthracene than for the TICT state of BA. This difference is attributed to the rate of back electron transfer from the primary radical pair to the molecular triplet state, which may be estimated on the basis of electron transfer theory.

Our analysis further asserts the role of complex formation between the primary radical pair and excess inorganic anion quenchers in the overall processes following primary electron transfer. The time dependence of the rate coefficients of bimolecular reactions appears to play an important role in the transient kinetics of fluorescence quenching and ISC induced by the quenching process.

Acknowledgements

This work was supported by the Swiss National Science Foundation and grant 1721/2/91 from the Polish State Committee for Scientific Research. The authors thank Dr Walter White III for the synthesis and purification of BA. M.M. wishes to thank the Swiss National Science Foundation for a fellowship under the project "Verstärkte Zusammenarbeit mit Osteuropäischen Staaten".

References

[1] Z.R. Grabowski, K. Rotkiewicz, A. Siemiarczuk, D.J. Cowley and W. Baumann, *Nouv. J. Chim., 3* (1979) 443; K. Rotkiewicz, K.H. Grellmann and Z.R. Grabowski, *Chem. Phys. Lett., 19* (1973) 315; Z.R. Grabowski and J. Dobkowski, *Pure Appl. Chem., 55* (1983) 315.

[2] P.F. Barbara and W. Jarzęba, *Adv. Photochem., 15* (1990) 1.

[3] D.W. Anthon and J.H. Clark, *J. Phys. Chem., 91* (1987) 3530.

[4] T.J. Kang, W. Jarzęba, P.F. Barbara and T. Fonseca, *Chem. Phys., 149* (1990) 87.

[5] N. Nakashima, M. Murakawa and N. Mataga, *Bull. Chem. Soc. Jpn., 49* (1976) 854.

[6] N. Mataga, H. Yao, T. Okada and W. Rettig, *J. Phys. Chem., 93* (1989) 3383.

[7] R. Kołos and Z.R. Grabowski, *J. Mol. Struct., 84* (1982) 251.

[8] H. Shizuka, M. Nakamura and T. Morita, *J. Phys. Chem., 84* (1980) 989; A.R. Watkins, *J. Phys. Chem., 78* (1974) 2555.

[9] H. Shizuka, Y. Ishi and T. Morita, *Chem. Phys. Lett., 51* (1977) 40.

[10] M. Mac, J. Wirz and J. Najbar, *Helv. Chim. Acta, 76* (1993) 1319.

[11] A. Treinin, I. Loeff, J.K. Hurley and H. Linschitz, *Chem. Phys. Lett., 95* (1983) 333; I. Loeff, A. Treinin and H. Linschitz, *J. Phys. Chem., 88* (1984) 4931; J.K. Hurley, H. Linschitz and A. Treinin, *J. Phys. Chem., 92* (1988) 5151; J. Loeff, W. Rabani, A. Treinin and H. Linschitz, *J. Am. Chem. Soc., 115* (1993) 8933.

[12] R.F. Föll, H.E. Kramer and U. Steiner, *J. Phys. Chem., 94* (1990) 2476.

[13] A. Magnus, H. Hartmann and F. Becker, *Z. Phys. Chem., 197* (1951) 75.

[14] M. Gisin and J. Wirz, *Helv. Chim. Acta, 66* (1983) 1556.

[15] T. Medinger and F. Wilkinson, *Trans. Faraday Soc., 61* (1965) 620.

[16] D.D.M. Wayner, in J.C. Scaiano (ed.), *Handbook of Organic Photochemistry*, Vol. II, CRC Press, Boca Raton, FL, 1988.
[17] I.V. Khudyakov, Y.A. Serebrennikov and N.J. Turro, *Chem. Rev., 93* (1993) 537.
[18] U.F. Steiner and T. Ulrich, *Chem. Rev., 89* (1989) 51.
[19] I.P. Gould, D. Ege, J.E. Moser and S. Farid, *J. Am. Chem. Soc., 112* (1990) 4290.
[20] J. Keizer, *Chem. Rev., 87* (1987) 167.
[21] J.N. Onuchic, *J. Chem. Phys., 87* (1987) 2090.
[22] R.A. Marcus, *J. Chem. Phys., 24* (1956) 966.
[23] M. Mac, J. Najbar, D. Phillips and T.A. Smith, *J. Chem. Soc., Faraday Trans., 88* (1992) 3001.
[24] M. Mac and J. Wirz, *Chem. Phys. Lett., 211* (1993) 20.
[25] H.A. Schwarz and B.H. Bielski, *J. Phys. Chem., 90* (1986) 1445.
[26] M.R. DeFillipis, M. Faraggi and M.H. Klapper, *J. Phys. Chem., 94* (1990) 2420.
[27] W. Rettig, *Angew. Chem., 98* (1986) 969.
[28] (a) D.J. Cowley and I. Pasha, *J. Chem. Soc., Perkin Trans. II*, (1983) 1139. (b) W. Rettig and M. Zander, *Z. Naturforsch., Teil A, 39* (1984) 41. (c) R.J. Visser, P.C.M. Weisenborn, J. Konijnenberg, B.H. Huizer and C.A.G.O. Varma, *J. Photochem., 32* (1986) 217. (d) G. Ponterini and J.C. Mialocq, *New J. Chem., 13* (1989) 157. (e) A. Gourdon, J.P. Launay, M. Bujoli-Doeuff, F. Heisel, J.A. Miehe, E. Amouyal and M.-L. Boillot, *J. Photochem. Photobiol. A: Chem., 71* (1993) 13. (f) G. Köhler, G. Grabner and K. Rotkiewicz, *Chem. Phys., 173* (1993) 275. (g) R. Günther, D. Oelkrug and W. Rettig, *J. Phys. Chem., 97* (1993) 8512.
[29] L. Salem and C. Rowland, *Angew. Chem., 84* (1972) 86; J. Michl, in S.J. Formosinho, I.G. Csizmadia and L.G. Arnaut (eds.), *Theoretical and Computational Models for Organic Chemistry*, Kluwer, Dordrecht, 1991, p. 207.
[30] J. Herbich and A. Kapturkiewicz, *Chem. Phys., 158* (1991) 143.
[31] S.L. Murov, *Handbook of Photochemistry*, Marcel Dekker, New York, 1973.